Mass Transfer of Dilute 1,2-Dimethoxyethane Aqueous Solutions During Pervaporation Process

Liang Liang,[1]* James M. Dickson,[1] Jianxiong Jiang,[2] Michael A. Brook[2]

[1]*Department of Chemical Engineering, McMaster University, Hamilton L8S 4L7, Canada*
[2]*Department of Chemistry, McMaster University, Hamilton L8S 4M1, Canada*

Received 16 March 2004; accepted 1 January 2005
DOI 10.1002/app.23056
Published online in Wiley InterScience (www.interscience.wiley.com).

ABSTRACT: Pervaporation of 1,2-dimethoxyethane (1,2-DME) is evaluated by crosslinked oligosilylstyrene–poly(dimethylsiloxane) composite membranes. A low flow velocity of the feed solution (1.0 L/min), corresponding to a Reynolds number of 220, is used. The pervaporation models are developed by combining the resistance in series and solution–diffusion models. The effects of the boundary layer on the performance of pervaporation are estimated by comparing experimental and theoretical data. The permeation fluxes of 1,2-DME and water fit very well with the calculated data from the models, but a deviation of the separation factor between the experimental and theoretical data is observed. © 2006 Wiley Periodicals, Inc. J Appl Polym Sci 100: 2075–2084, 2006

Key words: composite membrane; pervaporation; poly(dimethylsiloxane); 1,2-dimethoxyethane; boundary layer

INTRODUCTION

Compared with numerous works that developed pervaporation membranes and improved separation processes,[1–9] others studied the mass transfer of pervaporation by theoretical models.[10–19] Many theoretical treatments concerned the pervaporation of hydrophobic compounds, such as chlorinated and aromatic compounds.[10,20–22] A few theoretical models related to pervaporation of hydrophilic compounds with composite pervaporation membranes. 1,2-Dimethoxyethane (1,2-DME) is one hydrophilic compound that exhibits excellent miscible properties with water and is widely used as a solvent for organic synthesis,[23–26] a monomer and additive for polymerization,[27,28] and a cosolvent for batteries.[29,30] During these applications, wastewater contaminated with 1,2-DME is generated. In some cases, the amount of 1,2-DME in wastewater can be very low and the traditional separation methods, such as distillation and absorption, may not be efficient or economical. Therefore, the separation of 1,2-DME from dilute aqueous solution by pervaporation is important research work based on the considerations of environmental protection and energy conservation.

We previously studied the pervaporation of 1,2-DME by novel poly(dimethylsiloxane) (PDMS) composite membranes.[31] The composite membranes were prepared by casting solutions of H-terminated oligosilylstyrene (oligo-SiH_3) and vinyl-terminated PDMS (vinyl-PDMS) on the surface of a polysulfone (PSf) ultrafiltration membrane. The crosslinked PDMS gel was generated by the reaction of oligo-SiH_3 and vinyl-PDMS with a platinum complex as the catalyst. The composite membranes exhibited preferential selectivity to 1,2-DME. Depending on the operation conditions, the separation factor and the permeation flux of 1,2-DME are 55–184 and 0.31–3.3 g/m^2 h, respectively. It is interesting to study the mass transfer of 1,2-DME during pervaporation by theoretical models in order to predicate the performance of pervaporation and to manipulate the operation conditions. In the present study, we investigated the pervaporation of 1,2-DME by PDMS composite membranes, especially the effect of the top layer thickness on the separation performance. The theoretical models of pervaporation were developed by combining the resistance in series and solution–diffusion models. Moreover, a very low flow velocity of the feed solution (1.0 L/min), corresponding to a Reynolds number of 220, was utilized in this study. A low flow velocity of the feed solution can result in serious concentration polarization on the surface of membranes and subsequently poor pervaporation performance. Although the increase of the feed flow velocity is an effective method to improve the performance of pervaporation, the operation cost is increased because a higher power pump is used to maintain a high flow velocity during pervaporation.[12]

Correspondence to: L. Liang (liang2979@hotmail.com).
**Present address:* James Hardie Research USA LLC, 10901 Elm Avenue, Fontana, CA 92337.

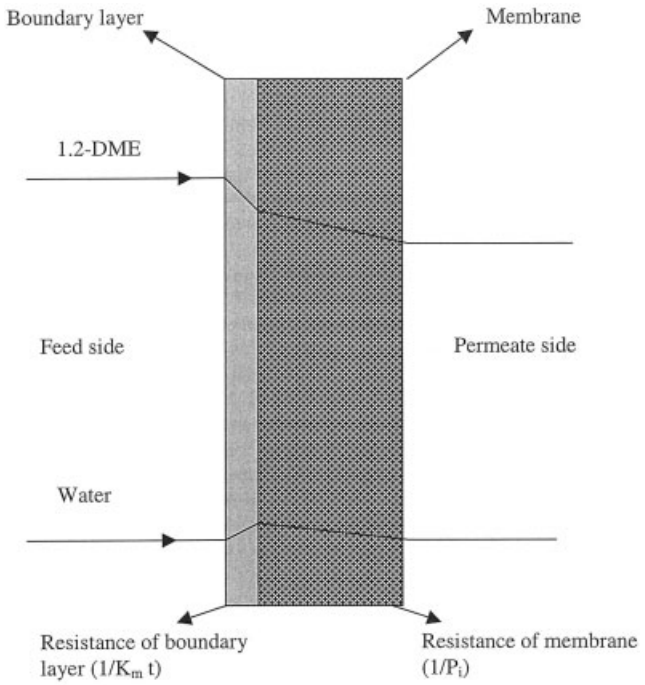

Figure 1 A schematic of the concentration profile for a 1,2-DME/water mixture solution during pervaporation in the presence of a boundary layer.

We also believe this study will benefit the understanding of pervaporation with the characteristics of serious concentration polarization and economical operation conditions for pervaporation.

THEORETICAL

Permeation flux

The solution–diffusion model shown in Figure 1 is frequently used to described the transport of permeates through a membrane by pervaporation.[10] During the solution–diffusion process, the components of a liquid mixture are first selectively absorbed at the upstream side of the membrane, then diffused through the membrane by the difference of the driving force, and are finally desorbed from the membrane as the vapor phase at the downstream side of the membrane. The permeation flux of organics (J_i) and water (J_w) in terms of their partial vapor pressure differences can be related to the downstream pressure, the compositions of the feed and permeate side, and the membrane thickness, as indicated in eqs. (1) and (2):

$$J_i = Q_i M_i (P_i^0 \gamma_i X_i - Y_i P_d)/t \quad (1)$$

$$J_w = Q_w M_w (P_w^0 \gamma_w X_w - Y_w P_d)/t \quad (2)$$

where Q_i and Q_w are the mass transfer coefficients of organics and water, respectively; P_i^0 and P_w^0 are the saturated vapor pressures of the organics and water [P_i^0(1,2-DME) = 5.8 kPa, 30°C; P_w^0(water) = 4.7 kPa, 30°C], respectively[32]; γ_i and γ_w are the activity coefficients of organics and water, respectively; and M_i and M_w are the molecular weights of the organics and water, respectively. For the purposes of simple calculation, we used the activity coefficient of tetrahydrofuran[33] (γ_i = 17) as that of 1,2-DME because of no public report on the activity coefficient of 1,2-DME to our knowledge and the two chemicals have similar structures and properties, which are shown in Figure 2 and Table I, respectively.[34] In addition, X_i and Y_i are the molar fractions of organics in the feed and the permeate, respectively, and X_w and Y_w are the molar fractions of water in the feed and the permeate, respectively. The membrane thickness is denoted as t and P_d is the pressure of the permeate side (or downstream pressure).

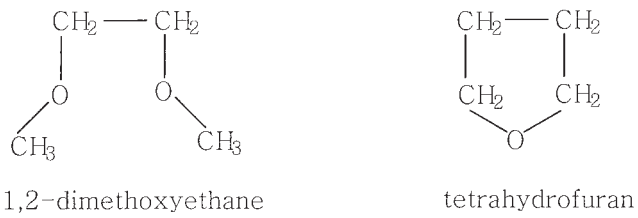

Figure 2 The chemical structures of 1,2-DME and tetrahydrofuran.

For the dilute aqueous solutions, it is reasonable that both the activity coefficient and the molar fraction of water are approximately equal to 1 ($\gamma_w \approx 1$, $X_w \approx 1$). Thus, eq. (2) can be rewritten as

$$J_w = Q_w M_w (P_w^0 - Y_w P_d)/t \quad (3)$$

Because the permeation flux of organics is much lower than that of water ($J_i \ll J_w$) in the cases of removing trace volatile organic compounds (VOCs) from aqueous solutions,[35,36] it is possible Y_w is much higher than Y_i because the permeation flux of compound i is proportional to the molar fraction of i in the vapor phase.[14] It might further be assumed that Y_w is near 1 and $Y_i P_d$ is near 0 in the case of an aqueous solution with trace VOCs and lower downstream pressure at the permeate side. Then, eqs. (1) and (3) can be rewritten as follows:

TABLE I
Properties of 1,2-Dimethoxyethane and Tetrahydrofuran

Chemical	bp (°C)	Density (g/cm^3)	Molecular weight (g/mol)
1,2-Dimethoxyethane	85	0.867	90
Tetrahydrofuran	67	0.889	72

$$J_i = Q_i M_i (P_i^0 \gamma_i X_i)/t \quad (4)$$

$$J_w = Q_w M_w (P_w^0 - P_d)/t \quad (5)$$

It has been shown experimentally that the concentration polarization can make a significance contribution to the overall mass transfer resistance, in particular for the removal of VOCs from dilute aqueous solutions.[15–18] Among various models, the resistance in series model can be effectively used to evaluate the transfer resistance at the boundary layer. According to this model, the overall mass transfer resistance ($1/Q_i$) consists of the sum of the membrane resistance ($1/P_i$) and the liquid boundary layer resistance ($1/K_m t$) as shown in Figure 1, where K_m and P_i are the mass transfer coefficients of the boundary layer and membrane, respectively. Many composite membranes are prepared by coating a polymer solution on the surface of a porous substrate such as a porous PSf ultrafiltration membrane. The membrane resistance consists of two parts: one from the top layer with a dense structure and another from the substrate with a porous structure. The resistance of the latter is much lower than that of the former because of the porous structure of the former. Therefore, the overall mass transfer resistance can be written as[20]

$$1/Q_i = 1/(K_m t) + 1/P_i \quad (6a)$$

or

$$t/Q_i = 1/K_m + t/P_i \quad (6b)$$

Substituting eq. (6b) into eq. (4), the permeation flux of organic compound can be expressed as

$$J_i = (P_i^0 \gamma_i X_i M_i)/(1/K_m + t/P_i)\,. \quad (7)$$

When the boundary layer resistance is negligible ($1/K_m + t/P_i \approx t/P_i$), we have

$$J_i = P_i M_i P_i^0 \gamma_i X_i/t\,. \quad (8)$$

If the boundary resistance dominates the overall mass transfer resistance ($1/K_m + t/P_i \approx 1/K_m$), we have

$$J_i = K_m M_i P_i^0 \gamma_i X_i\,. \quad (9)$$

Separation factor

The separation factor (α), which indicates the enrichment in the preferentially permeating compound through the membranes, can be generally defined as[2]

$$\alpha = [Y_i/(1 - Y_i)]/[X_i/(1 - X_i)] \quad (10)$$

where Y_i and X_i are the molar fractions of organic compounds in the permeate side and the feed solution. Because of the molar fraction of the organic compound in the vapor phase, Y_i can be taken as the ratio of the organic component flux over the total flux. Thus, we have

$$Y_i = J_i/J_0 \quad (11)$$

where $J_0 = J_i + J_w$. Usually, the permeation flux of water is much higher than that of an organic compound during pervaporation to remove trace VOCs from a dilute liquid solution, that is, $J_w \gg J_i$; so we have

$$Y_i = J_i/J_w \quad (12)$$

Substituting eqs. (4), (5), and (12) into eq. (10), an expression for the separation factor is obtained as a function of the feed composition, downstream pressure, and mass transfer coefficient of components:

$$\alpha = \{{}_i M_i (P_i^0 \gamma_i X_i)/[Q_i M_i (P_i^0 \gamma_i X_i) + Q_w M_w (P_w^0 - P_d)]\}/[X_i/(1 - X_i)] \quad (13)$$

With the condition of $J_w \gg J_i$, eq. (13) can be rewritten as

$$\alpha = Q_i M_i P_i^0 \gamma_i (1 - X_i)/[Q_w M_w (P_w^0 - P_d)] \quad (14)$$

Combining eqs. (6a) and (14), we get

$$\alpha = \{M_i P_i^0 \gamma_i (1 - X_i)/[Q_w M_w (P_w^0 - P_d)]\} \times [1/(tK_m) + 1/P_i] \quad (15)$$

Furthermore, if the boundary resistance is negligible, we find

$$\alpha = P_i \{M_i P_i^0 \gamma_i (1 - X_i)/[Q_w M_w (P_w^0 - P_d)]\} \quad (16)$$

If the boundary resistance dominates the overall resistance, we have

$$\alpha = \{M_i P_i^0 \gamma_i\, (1 - X_i)/[Q_w M_w (P_w^0 - P_d)]\} K_m t \quad (17)$$

EXPERIMENTAL

Materials

Vinyl-PDMS (Hülser–Petrach), platinum divinyltetramethyldisiloxane complex (Pt catalyst, 3% in toluene, Gelest), hexane (99%, Fisher), and 1,2-DME (99%, Fisher) were received and used without further purification. Deionized water was used in all experiments. The preparation procedure of oligo-SiH_3 was reported in previous articles.[12,37] We used PSf ultrafiltration

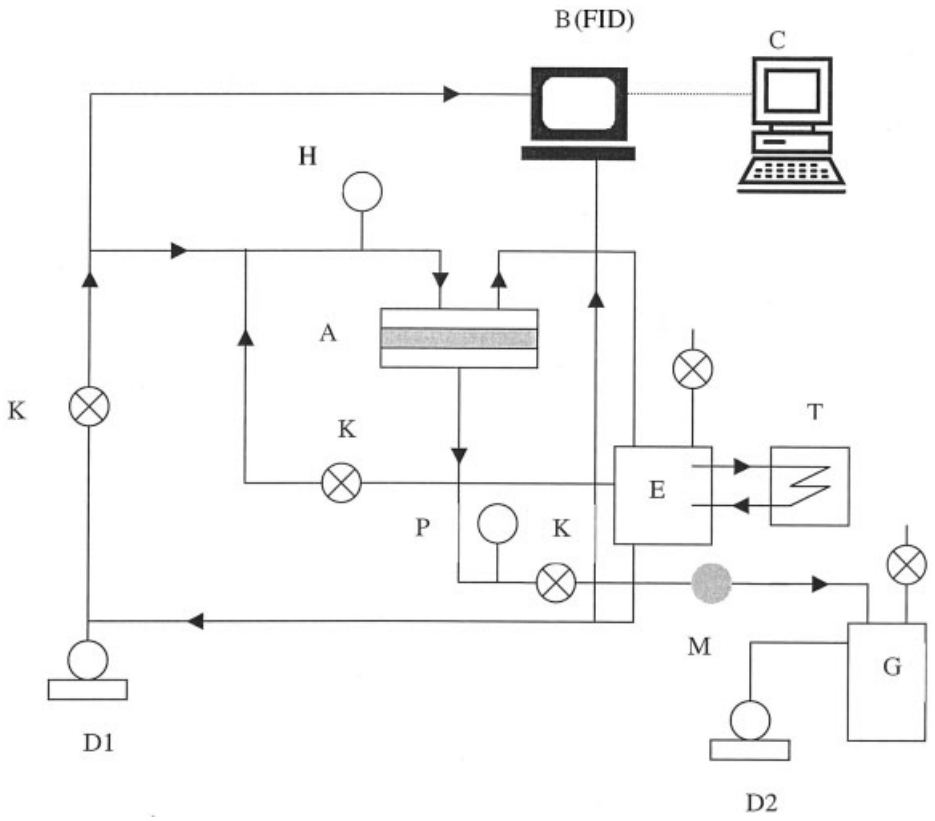

Figure 3 A schematic of the pervaporation apparatus: A, pervaporation cell; B, gas chromatograph; C, computer; D1, recirculating pump; D2, vacuum pump; E, feed tank; F, thermostat; G, cold trap; H, temperature transducer; T, thermocouple; P, pressure transducer; M, mass flow meter; K, control valve.

membranes (U.S. Filter) as support membranes. The PSf membranes have characteristics to separate dextran with a molecular weight of 100,000 and have nonwoven polypropylene as the bottom layer. The thickness of the PSf membranes is about 175 μm, which was measured by a micrometer with an error range of $\pm$5%. The PSf membranes were dipped in isopropanol overnight to remove chemicals inside the membranes and dried completely in a hood for 1 day.

Preparation of composite membranes

Vinyl-PDMS solution (20 wt %) containing 0.2 mL of Pt catalyst was prepared by dissolving 1.0 g of vinyl-PDMS (viscosity = 500 cs) in 5 mL of hexane. Oligo-SiH_3 solution (20 wt %) was prepared by dissolving 0.2 g of oligo-SiH_3 in 1 mL of hexane. Then, these two solutions were mixed with a magnetic stirrer for 0.5 h at room temperature. The mixture solution was poured onto the surface of PSf membranes that were clamped into the pervaporation cell, and the solvent was allowed to evaporate at room temperature overnight. Subsequently, the membranes were dried in an oven at 100°C for an additional 8 h. A micrometer with an error range of $\pm$5 μm was used to measure the thickness of the final composite membrane. The thickness of the top layer was calculated by subtracting the thickness of the PSf membrane from the overall thickness of the composite membrane. The average thickness of the top layer was obtained from the measurements of five points on each membrane. Composite membranes with top layer thicknesses ranging from 39 to 157 μm were used in this study.

Pervaporation

Figure 3 provides a schematic of the pervaporation equipment. The feed solution was cycled between the feed tank and pervaporation cell using a cycling pump. Composite membranes with an effective area of 31.2 cm^2 were clamped into the pervaporation cell. The feed temperature was controlled by a thermocouple (T), and the downstream pressure was monitored with a pressure transducer (P). The feed flow velocity was measured with a mass flow meter (M). The concentrations of the feed and the permeate were measured by a gas chromatograph (HP 5890) equipped with a flame ionization detector (FID) and a Porapak P column heated at 150°C. All operating parameters were monitored and recorded by a computer (C). The data of the permeation flux, the compositions of the feed, and the permeate side were collected after at

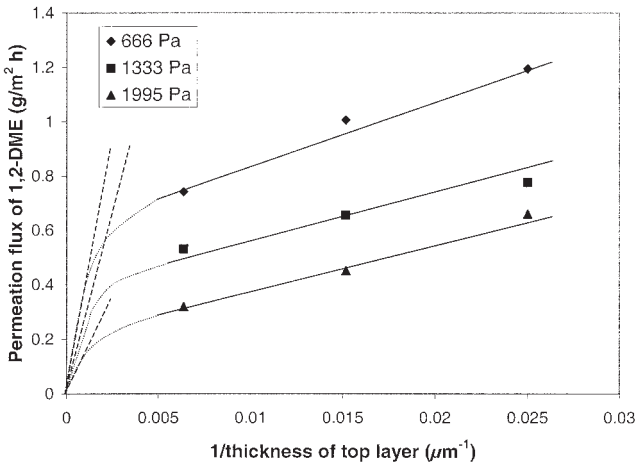

(a)

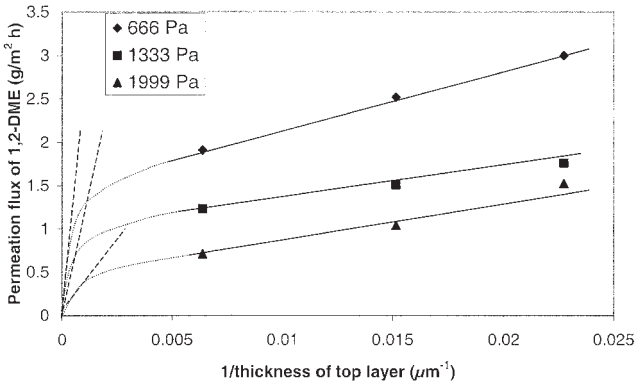

(b)

Figure 4 The permeation flux of 1,2-DME versus the reverse thickness of the top layer; feed temperature = 30°C; feed composition of 1,2-DME in water = (a) 120 and (b) 737 ppm.

least 3 h of separation once a steady state was achieved. The error range of the permeation flux and separation factor are 3 and 10%, respectively, with 95% confidence.

RESULTS AND DISCUSSION

Mass transfer coefficients of 1,2-DME and water

Figure 4 shows the relationship between the reverse thickness of the top layer and the permeation flux of 1,2-DME. The feed temperature was kept at 30°C and the concentration of 1,2-DME in the feed was changed from 120 to 737 ppm. The deviation of the permeation flux from Fick's diffusion law[38] is observed for the membranes with thinner top layesr, which is indicated as solid lines in Figure 4. The reason for the deviation is the presence of a boundary layer generated by the concentration polarization of 1,2-DME between the feed solution and the adjoining area with the membrane. Although there is excellent miscibility of 1,2-DME with water, the different selectivities of the composite membranes to 1,2-DME and water can result in the difference of the permeation flux between 1,2-DME and water. The preferable selectivity of composite membranes to 1,2-DME produced a faster transfer of 1,2-DME through the membrane and an area with low concentration of 1,2-DME could be generated on the membrane surface, as shown in Figure 1. The transfer resistance of the boundary layer can be neglected if compared with the transfer resistance of the membrane with a thicker top layer. Therefore, the overall transfer resistance will come from the membrane and the permeation flux of 1,2-DME will follow Fick's diffusion law, which is shown by dotted lines in Figure 4. Figure 5 shows that the permeation flux of water almost follows Fick's diffusion law. It is reasonable that there is no boundary layer effect on the transfer of water through the membranes.

According to eq. (5), Q_w can be obtained from the slope of the straight line as shown in Figure 5. Table II collects the Q_w data at various feed concentrations and downstream pressures. The mass transfer coefficient of water increases a little with increasing of the downstream pressure, as expected by eq. (5). Table III summarizes the mass transfer coefficients of water re-

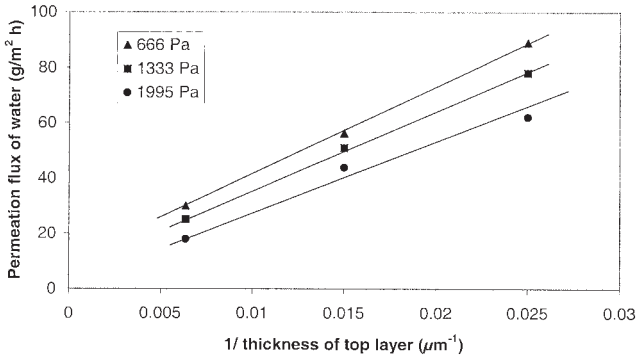

(a)

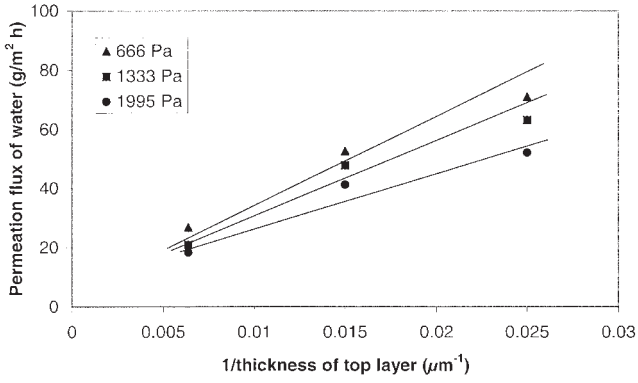

(b)

Figure 5 The permeation flux of water versus the inverse thickness of the top layer; feed temperature = 30°C; feed composition of 1,2-DME in water = (a) 120 and (b) 737 ppm.

TABLE II
Mass Transfer Coefficient of Water (30°C)

Feed concn of 1,2-DME (ppm)	Downstream pressure (Pa)	Q_w (mol m/m^2 kPa s)
120	666	1.399×10^{-8}
	1333	1.481×10^{-8}
	1995	1.489×10^{-8}
737	666	1.173×10^{-8}
	1333	1.248×10^{-8}
	1995	1.305×10^{-8}

The thickness of the top layer ranges from 39 to 157 μm. Linear regression coefficients are >98%. Q_w, mass transfer coefficient of water.

ported in the literature[39–41] for comparison purposes. It can be seen the mass transfer coefficient of water obtained in this study is close to those published by others. When plotting t/Q_i versus t as described in eq. (6b), the K_m and P_i can be obtained from the intercept and slope of the straight line, respectively. Figure 6 shows typical plots between t/Q_i and t, and Table IV lists the mass transfer coefficients of the membrane and boundary layer at different feed concentrations and downstream pressures, which are used to further calculate the permeation flux and separation factor based on developed mass transfer models.

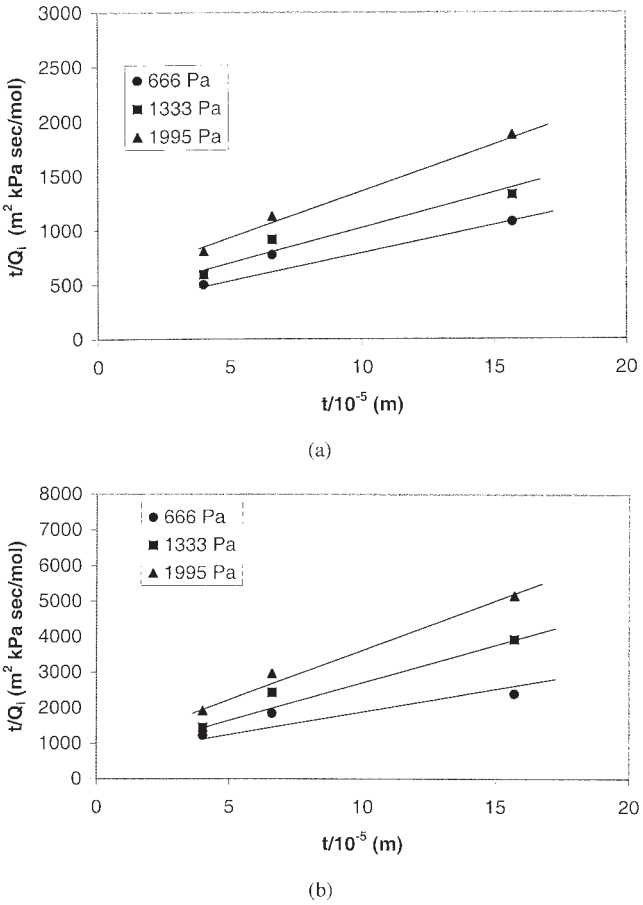

Figure 6 The relationship between t/Q_i and t; feed composition of 1,2-DME in water = (a) 120 and (b) 737 ppm; feed temperature = 30°C.

Permeation flux of 1,2-DME

Figure 7 shows the dependence of the permeation flux of 1,2-DME on the inverse thickness of the top layer with or without the boundary layer under a downstream pressure of 666 Pa and a feed temperature of 30°C. The solid straight lines are plotted by eq. (7) with a boundary layer. The dotted lines were obtained by eq. (8) without a boundary layer. The solid black points are experimental data and they fit the theoretical data very well, which confirms the presence of the boundary layer. The permeation flux of 1,2-DME without a boundary layer is almost 14 times higher than that with a boundary layer when the thickness of the top layer is 20 μm. With an increase of the top layer thickness, the difference between the permeation flux with and without a boundary layer decreased. This is because the contribution of the boundary layer resistance to the overall resistance decreased as the thickness of the top layer increased.

TABLE III
Mass Transfer Coefficient of Water Reported in Literature

Membrane	Temp. (°C)	Membrane thickness (μm)	Q_w (mol m/m^2 kPa s)	Reference
PDMS	22	165	1.12×10^{-8}	17
PDMS	30	140	2.32×10^{-8}	47
PDMS	22	165	1.12×10^{-8}	48
PEBA	50	70	1.23×10^{-8}	49
PEBA	30	27	8.30×10^{-9}	48
PUR	30	38	5.90×10^{-9}	48
SPC	30	23	4.70×10^{-9}	48
PDMS	30	39–157	1.35×10^{-8}	This study

Q_w, mass transfer coefficient of water.

TABLE IV
Mass Transfer Coefficients of Membrane and Boundary Layer (30°C)

Downstream pressure (Pa)	Feed concn (ppm)	P_i (mol m/m^2 kPa s)	K_m (mol/m^2 kPa s)
666	120	3.38×10^{-7}	1.06×10^{-3}
	271	3.59×10^{-7}	5.87×10^{-4}
	423	1.39×10^{-7}	1.35×10^{-4}
	737	1.19×10^{-7}	6.69×10^{-5}
1333	120	1.72×10^{-7}	2.28×10^{-3}
	271	1.99×10^{-7}	1.39×10^{-3}
	423	6.50×10^{-8}	3.23×10^{-4}
	737	6.20×10^{-8}	1.55×10^{-4}
1995	120	1.12×10^{-7}	3.04×10^{-3}
	271	1.14×10^{-7}	2.22×10^{-3}
	423	4.53×10^{-8}	4.46×10^{-4}
	737	3.73×10^{-8}	2.42×10^{-4}

The thickness of the top layer ranges from 39 to 157 μm. Linear regression coefficients are >98%. P_i, mass transfer coefficient of membrane; K_m, mass transfer coefficient of boundary layer.

Permeation flux of water

Figure 8 shows the effect of the top layer thickness on the permeation flux of water. The solid lines represent the theoretical data calculated by eq. (5) and the solid black points are the experimental data. It can be seen from Figure 8 that the permeation flux of water decreased with the increase of the top layer thickness. The decrease of the water permeation flux is the reason that the transfer resistance of water increased with the increase of the membrane thickness. Figure 9 shows the effect of the downstream pressure on the permeation flux of water for the membrane with a different top layer thickness. The solid line is plotted by the data calculated from eq. (5) and the solid black points are the experimental results. The permeation flux of water decreased linearly with the increase of the downstream pressure. This is because the driving force of water through the membrane was decreased by the increase of the downstream pressure. The permeation flux of water is close to zero by exploring the solid lines on the Y axis. At this point, the partial vapor pressure of water at the permeate side is equal to the downstream pressure as indicated by eq. (5).

Separation factor

Figure 10 shows the effect of the inverse thickness of the top layer on the separation factor with or without a boundary layer under a downstream pressure of 666 Pa and a feed temperature of 30°C. The theoretical data calculated by eq. (15) with a boundary layer and by eq. (16) without a boundary layer are represented by solid and dotted lines, respectively, for comparison purposes. The separation factor without a boundary layer is constant and higher than those with a boundary layer, as shown in Figure 10. It is clear that the

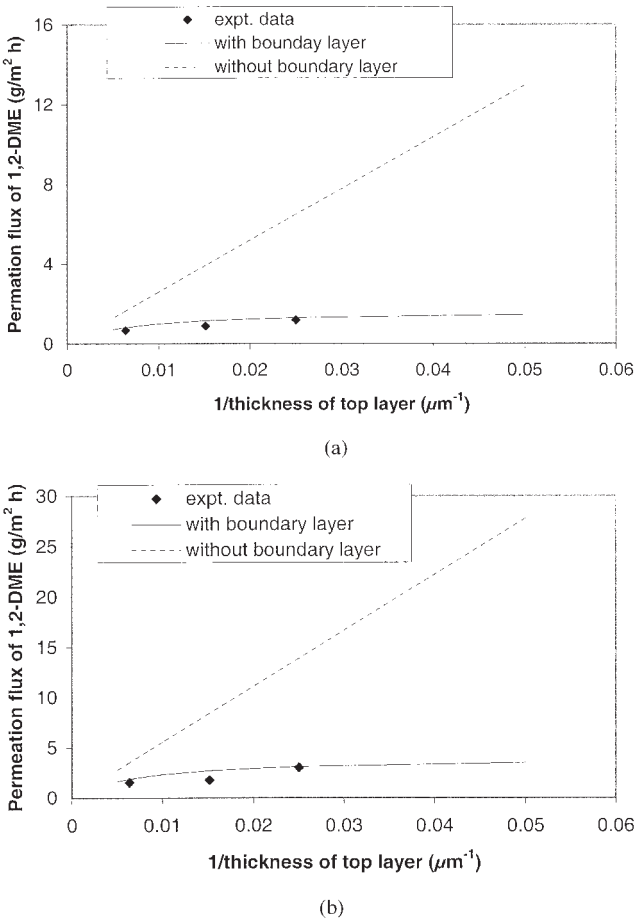

Figure 7 The permeation flux of 1,2-DME versus the reverse thickness of the top layer; feed temperature = 30°C; downstream pressure = 666 Pa, feed composition of 1,2-DME in water = (a) 120 and (b) 737 ppm.

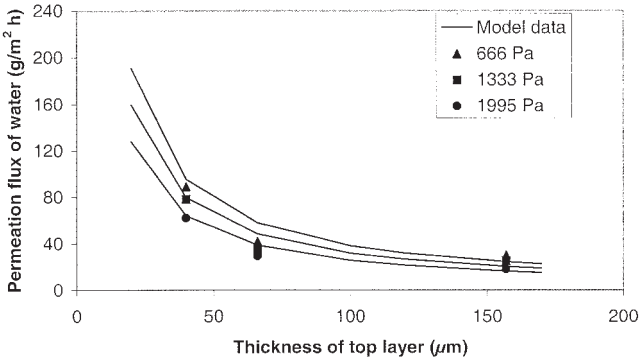

Figure 8 The permeation flux of water versus the reverse thickness of the top layer; feed temperature = 30°C; downstream pressure = 666 Pa; feed composition of 1,2-DME in water = 120 ppm.

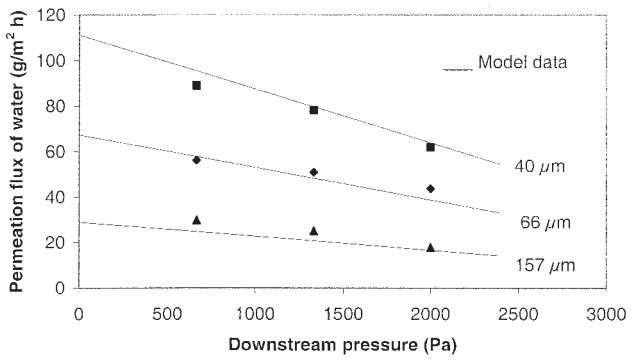

Figure 9 The permeation flux of water versus the downstream pressure; feed temperature = 30°C; feed composition of 1,2-DME in water = 120 ppm.

presence of a boundary layer results in the decrease of both the permeation flux of 1,2-DME and the separation factor. The decrease of the separation factor can be attributed to the fact that the permeation flux of 1,2-DME decreased with the presence of the boundary layer. The difference in the separation factor with and without boundary layers is reduced as the thickness of the top layer increased because the effect of the boundary layer on the permeation flux of 1,2-DME becomes less significant for the membrane with a thicker top layer.

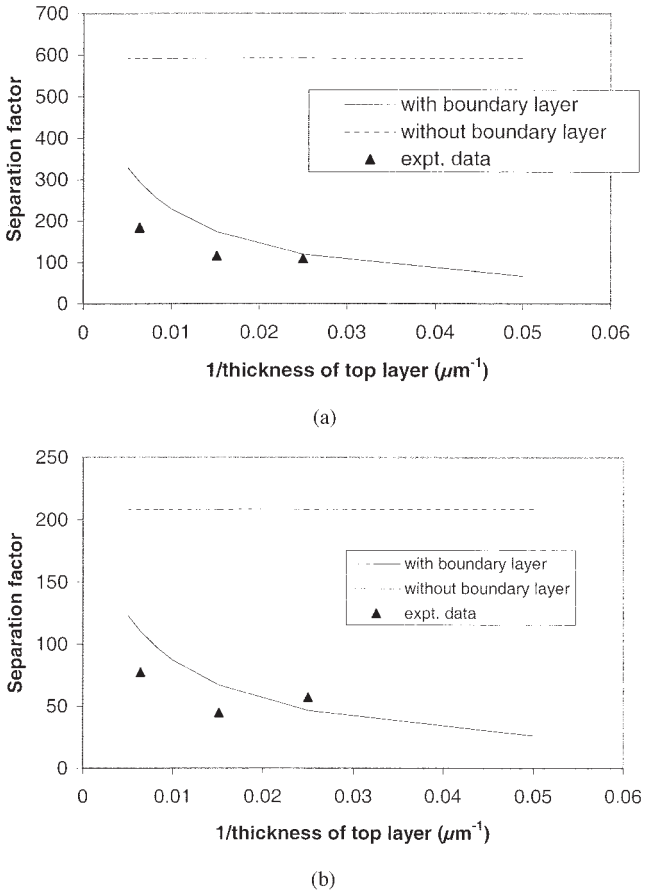

Figure 10 The separation factor versus the inverse thickness of the top layer; feed temperature = 30°C; downstream pressure = 666 Pa; feed composition of 1,2-DME in water = (a) 120 and (b) 737 ppm.

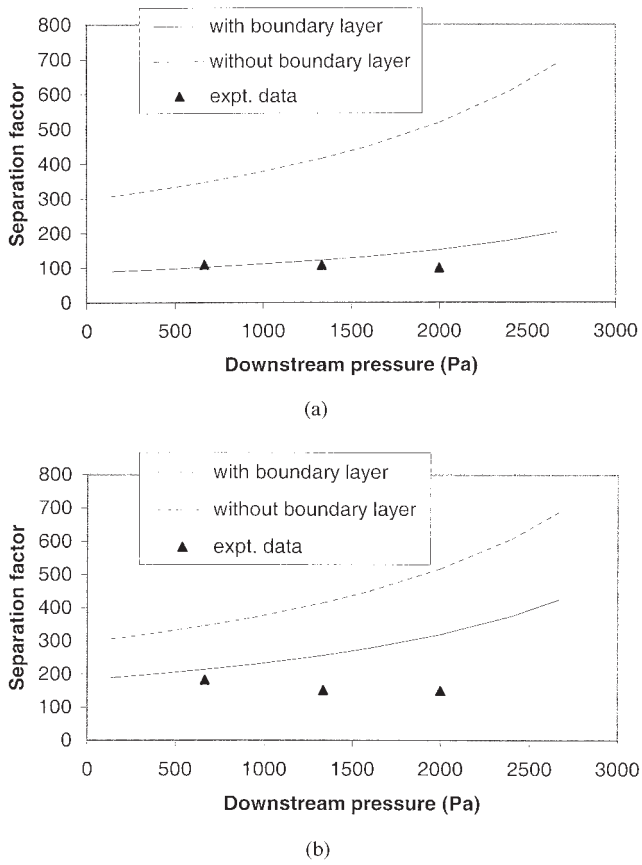

Figure 11 The separation factor versus the downstream pressure; feed temperature = 30°C; feed composition of 1,2-DME in water = 120 ppm; membrane thickness = (a) 39 and (b) 157 μm.

The change of the separation factor with the downstream pressure at a feed temperature of 30°C and a feed composition of 120 ppm is presented in Figure 11. The solid and dotted lines are drawn by eqs. (15) and (16), respectively, which indicate the effect of the downstream pressure on the separation factor with or without a boundary layer. Based on eqs. (15) and (16), the separation factor will be increased with increasing downstream pressure, which is consistent with the results shown in Figure 11. Figure 11(b) shows a deviation between the experimental and calculated data for the membrane with a thicker top layer at higher downstream pressure. The deviation could be the reason that the resistance of the permeate side is neglected in the developed theoretical models; however, it would be incorrect for the membranes with a thicker top layer and processed at higher downstream pressure.

CONCLUSIONS

The effect of a boundary layer on the mass transfer of dilute 1,2-DME aqueous solutions was observed during the pervaporation of the composite membranes from crosslinked PDMS as the top layer and PSf ultrafiltration membrane as the substrate. The theoretical models developed from the resistance in series and solution–diffusion models effectively described the mass transfer of 1,2-DME aqueous solutions during pervaporation with various feed concentrations and downstream pressures. The top layer thickness of composite membranes was a critical factor to control the effect of the boundary layer. The permeation flux of 1,2-DME without a boundary layer was 14 times higher than that with a boundary layer when the thickness of the top layer was about 20 μm. However, the difference between the permeation flux of 1,2-DME with or without a boundary layer was reduced to 1.5 times when the thickness of the top layer was about 160 μm. The permeation flux of water was independent of the presence of a boundary layer and the increase of the water permeation flux through the thinner membranes was attributed to the decrease of the membrane resistance. The theoretical data of both permeation flux and separation factor with a boundary layer fit with the experimental data very well, which implied that the characteristics of pervaporation could be predicted and the performance of separation could be manipulated. Larger deviations between the theoretical and experimental data of the separation factor were observed when the membrane with a thicker top layer was used and higher downstream pressure was maintained. The assumptions that the resistance of the permeate side could be neglected might not be reasonable for membranes with thicker top layers and processed at higher downstream pressures.

We appreciate the support from the Ministry of Economic Development and Trade, Ontario, Canada, and the National Science and Technology Board of Singapore.

NOMENCLATURE

Variables

K_m mass transfer coefficient of boundary layer (mol/m^2 kPa s)
J_i permeation flux of 1,2-DME (g/m^2 h)
J_w permeation flux of water (g/m^2 h)
M_i molecular weight of organics
M_w molecular weight of water
P_i^0 saturated vapor pressure of 1,2-DME (kPa)
P_w^0 saturated vapor pressure of water (kPa)
P_d downstream pressure (Pa)
P_i mass transfer coefficient of membrane (mol m/m^2 kPa s)
Q_i mass transfer coefficient of 1,2-DME (mol m/m^2 kPa s)
Q_w mass transfer coefficient of water (mol m/m^2 kPa s)
t membrane thickness (μm)
X_i molar fraction of 1,2-DME in the feed
X_w molar fraction of water in the feed
Y_i molar fraction of 1,2-DME in the permeate
Y_w molar fraction of water in the permeate

Greeks

α separation factor
γ_i activity coefficient of 1,2-DME
γ_w activity coefficient of water

References

1. Won, W.; Feng, X.; Lawless, D. J Membr Sci 2002, 209, 493.
2. Winston Ho, W. S.; Sirkar, K. K., Eds. Membrane Handbook; Van Nostrand Reinhold: New York, 1992; Chapter 3.
3. Aminabhavi, T. M.; Khinnavar, R. S.; Harogoppad, R. S.; Aithal, U. S.; Nguyen, Q. T.; Hansen, K. C. J. Macromol Chem Phys 1994, 34, 139.
4. Rautenbach, R.; Albrech, R. Membrane Process; Wiley: Wiltshire, U.K., 1989.
5. Bluemke, W.; Schrader, J. Biomol Eng 2001, 17, 137.
6. Rhim, J. W.; Sohn, M. Y.; Lee, K. H. J Appl Polym Sci 1994, 52, 1217.
7. Reyes, F. D.; Romero, J. M. F.; de Castro, M. D. L. Anal Chim Acta 2001, 434, 95.
8. Zhang, S.; Drioli, E. Sep Sci Technol 1995, 30, 1.
9. Hernández, J. A.; de Castro, M. D. L. Food Chem 2000, 68, 387.
10. Raghunath, B.; Hwang, S. T. J Membr Sci 1992, 65, 147.
11. Ji, W. C.; Sikdar, S. K.; Hwang, S. T. J Membr Sci 1994, 93, 1.
12. Ji, W. C.; Hilaly, A.; Sikdar, S. K.; Hwang, S. T. J Membr Sci 1995, 97, 109.
13. Wijmans, J. G.; Baker, R. W. J Membr Sci 1995, 107, 1.
14. Côté, P.; Lipski, C. In Proceedings of the 3rd International Conference on Pervaporation Processes in the Chemical Industry; Bakish, R., Ed.; Bakish Materials Corp.: Englewood, NJ, 1988; p 449.
15. Bhattacharya, S.; Hwang, S. T. J Membr Sci 1997, 132, 73.
16. Gref, R.; Nguyen, Q. T.; Neel, J. Sep Sci Technol 1992, 27, 467.
17. Nijhuis, H. H.; Mulder, M. H. V.; Smolders, C. A. J Membr Sci 1991, 61, 99.
18. Heintz, A.; Stephan, W. J Membr Sci 1994, 89, 153.
19. Cao, B.; Henson, M. A. Annals NY Acad Sci 2003, 984, 370.
20. Marriott, J.; Sorensen, E. A. Chem Eng Sci 2003, 58, 4975.
21. Izak, P.; Bartovska, L.; Friess, K.; Sipek, M.; Uchytil, P. Polymer 2003, 44, 2679.
22. Ghoreyshi, A. A.; Farhadpour, F. A.; Soltanieh, M.; Bansal, A. J Membr Sci 2003, 211, 193.
23. Deacon, G. B.; Delbridge, E. E.; Skelton, B. W.; White, A. H. Eur J Inorg Chem 1998, 5, 543.
24. Schareina, T.; Hillebrand, G.; Fuhrmann, H.; Kempe, R. Eur J Inorg Chem 2001, 9, 2421.
25. Steiger, B.; Anson, F. C. J Porphy Phthalo 1999, 3, 159.
26. Smith, G. D.; Borodin, O.; Bedrov, D. J Comput Chem 2002, 23, 1480.
27. Narita, T.; Hagiwara, T.; Hamana, H. Macromol Chem Phys 2000, 201, 220.

28. Liang, L.; Ying, S. K. Makromol Chem 1993, 194, 581.
29. Martins, L.; Aeiyach, S.; Jouini, M.; Lacaze, P. C.; Satge, J.; Martins, J. P. Appl Organomet Chem 2002, 16, 76.
30. Xu, J.; Farrington, G. C. J Electrochem Sci 1995, 142, 3303.
31. Liang, L.; Dickson, J. M.; Jiang, J.; Brook, M. A. J Appl Polym Sci 2004, 92, 2284.
32. Yaws, C. L. Thermodynamic and Physical Property Data; Gulf Publishing Co.: Houston, 1992; p 79.
33. Zhang, S.; Hiaki, T.; Kojima, K. Fluid Phase Equilib 2002, 198, 15.
34. Lide, D. R., Ed. Handbook of Chemistry and Physics; CRC Press: New York, 1995.
35. Athayder, A. L.; Baker, R. W.; Danieles, R.; Le, M. H.; Ly, J. H. ChemTech 1997, 27, 34.
36. Feng, X.; Huang, R. Y. M. Ind Eng Chem Res 1997, 36, 1048.
37. Brook, M. A.; Hulser, P.; Sebastian, T. Macromolecules 1989, 22, 3814.
38. Atkins, P. W. Physical Chemistry; W.H. Freeman; New York, 1985; Chapter 26.
39. Hall, C. Polymer Materials; Wiley: New York, 1980; Chapter 2.
40. Psaume, R.; Aptel, Ph.; Aurelle, Y.; Mora, J. C.; Bersillon, J. L. J Membr Sci 1988, 36, 373.
41. Böddeker, K. W.; Bengston, G.; Bode, E. J Membr Sci 1990, 53, 143.